Upregulation of SGOL2 Predicts Poor Prognosis and Facilitates Hepatocellular Carcinoma Progression via Dysregulating the Cell Cycle by Directly Activating MAD2

Qingqing Hu
Zhejiang University School of Medicine First Affiliated Hospital
Xiaochu Hu
Nanjing Medical University
Yalei Zhao
Zhejiang University School of Medicine First Affiliated Hospital
Lingjian Zhang
Zhejiang University School of Medicine First Affiliated Hospital
Ya Yang
Zhejiang University School of Medicine First Affiliated Hospital
lanjuan li (ljli@zju.edu.cn)
Zhejiang University First Affiliated Hospital State Key Laboratory for Diagnosis and Treatment of Infectious Diseases

Research

Keywords: SGOL2, MAD2, Cell cycle, Hepatocellular carcinoma

Posted Date: June 8th, 2021

DOI: https://doi.org/10.21203/rs.3.rs-560609/v1

Abstract

Background: Hepatocellular carcinoma (HCC) is the third leading cause of cancer-related death worldwide. Shugoshin-like protein 2 (SGOL2) is a centromeric protein that ensures the correct and orderly process of mitosis by protecting and maintaining centripetal adhesions during meiosis and mitosis. However, the role of SGOL2 in cancer is not well understood.

Methods: The mRNA and protein levels of SGOL2 and survival analysis were conducted in The Cancer Genome Atlas (TCGA) and further validated in 2 independent cohorts. Differential genes correlated with SGOL2 and mitotic arrest deficient 2 like 1 (MAD2) were obtained using LinkedOmics. Subsequently, loss-of-function and rescue assays were carried out in vitro and in vivo to assess the functions of SGOL2 in hepatic tumorigenisis.

Findings: We found that SGOL2 was significantly overexpressed in HCC and predicted unfavorable overall survival in HCC patients. Next, we identified 47 differentially expressed genes positively correlated with both SGOL2 and MAD2 to be mainly involved in the cell cycle. In addition, SGOL2 downregulation suppressed the migration, invasion, proliferation, stemness and EMT of HCC cells and inhibited tumorigenesis in vivo. Furthermore, SGOL2 promoted tumor proliferation by activating MAD2-induced cell cycle dysregulation, which could be reversed by the MAD2 inhibitor M2I-1. We also proved that SGOL2 activated MAD2 by directly binding with MAD2.

Conclusions: The results of this study showed that SGOL2 acts as an oncogene in HCC cells by directly activating MAD2 and then dysregulating the cell cycle, thereby providing a potential target for HCC patients in the future.

Background

Hepatocellular carcinoma, a major type of primary liver cancer, is the third leading cause of cancer-related mortality worldwide[1]. Despite recent improvements in the diagnosis and treatment strategies for HCC, the prognosis of HCC patients and the treatment options for patients with advanced liver cancer are still far from satisfactory when compared with those of other types of tumors[2, 3]. Hence, there is an urgent need to identify novel biomarkers for the early diagnosis and progression of HCC.

During cell mitosis, the precise separation of chromosomes is critical for the maintenance of genomic stability and function[4, 5]. Genetic instability caused by chromosomal abnormalities may contribute to a variety of diseases, including cancers[6]. Shugoshins, including SGOL1 and SGOL2, were originally considered to be protectors of centromeric cohesion during meiosis and mitosis, which is fundamental for both chromatin structure and function[7, 8]. During the M phase of the cell cycle, shugoshins recruit PP2A to the centromere and act as a centromeric adaptor for protein phosphatase 2 A (PP2A)[9–12]. Shugoshin-like protein 2 (SGOL2) is a centromeric protein that associates with cohesin at centromeres and ensures the correct and orderly conduct of mitosis by protecting and maintaining centripetal

adhesions during meiosis and mitosis[13, 14]. SGOL2 is also reportedly associated with chromatin condensation and the transcription of subtelomere genes[15]. As previously reported, SGOL2 specifically interacts with mitotic arrest deficient 2 like 1 (MAD2) and regulates the processes of cell mitosis[16], especially in the separation of eukaryotic sister chromatids. In general, SGOL2 could form a SGOL2–MAD2 complex upon binded with SAC-activated MAD2, which function together as a separase inhibitor[16]. In addition, activated MAD2 enables SGOL2 to bind and sequester separase through cell cycle[16]. Therefore, the proper expression of SGOL2 is essential for maintaining normal physiological conditions, whereas the abnormal expression of SGOL2 can lead to the occurrence of disease. For example, R. Faridi reported that Perrault syndrome could be collectively caused by comutations of SGOL2 and CLDN14[17]. In addition, SGOL2 plays a critical role in tumorigenesis. A study from Canada demonstrated that the expression of SGOL2 was significantly different in Sézary syndrome patients compared to the healthy[18]. However, no one knows how SGOL2 functions in HCC. Thus, further research on SGOL2 is urgently needed.

The aim of this study was to explore the biological function of SGOL2 in HCC through bioinformatics analysis and to clarify its probable mechanisms. We used a variety of informatics tools to evaluate its expression profile, which was further verified in 2 independent HCC cohorts. We also found that SGOL2 promoted HCC progression in vitro and in vivo. Further investigation demonstrated that SGOL2 can activate MAD2 by directly binding with MAD2, which subsequently induced cell cycle dysregulation in HCC cells. Thus, the results of this study further our knowledge of SGOL2 and highlight its potential as a new therapeutic target for hepatocellular carcinoma.

Methods

2.1 Clinical specimens

A total of 199 paracancerous normal HCC tissues and 202 HCC tissues were collected in this study. One part of the samples was obtained from Shanghai Outdo Biotech Company (Shanghai, China), Cohort 1 (97 pairs of matched HCC and normal paracancerous tissues and 3 single HCC tissues). The other part was from the Department of Hepatobiliary Surgery, the First Affiliated Hospital of Zhejiang University (Zhejiang, China), Cohort 2 (102 pairs of matched HCC and normal paracancerous tissues). The clinicopathological characteristics of all patients are shown in supplement Table 1 (Cohort 1) and Table 2 (Cohort 2).

2.2 Expression analysis

The mRNA level of SGOL2 in tumor versus normal tissues and liver cancer versus normal liver tissues was analyzed using the websites Gene Expression Profiling Interactive Analysis (GEPIA) and Oncomine. The protein level of SGOL2 in HCC was analyzed in the Human Protein Atlas (HPA) database and verified in Cohort 2 by Western blot and Cohort 1/2 by immunohistochemistry (IHC) staining. Next, we performed subgroup analysis of SGOL2 mRNA expression using the liver hepatocellular carcinoma (LIHC) dataset

from The Cancer Genome Atlas (TCGA) and the UALCAN database. We also analyzed the mRNA expression levels of SGOL2 in various cell lines, including seventeen liver cell lines in CCLE database.

2.3 Survival analysis

We performed Kaplan-Meier analysis for overall survival (OS), relapse-free survival (RFS), progression-free survival (PFS), and disease-specific survival (DSS) in the Kaplan-Meier Plotter database. In addition, patients in Cohort 1 were separated into low- and high-expression groups according to the median expression value of SGOL2. Then, we performed overall survival analysis, and the log-rank test was used to compare survival curves. Moreover, multivariate Cox proportional hazards regression analyses were performed to test whether SGOL2 was an independent prognostic factor in R software 3.6.0.

2.4 Mutation and immune infiltration analysis

We assessed the mutation types and frequencies of SGOL2 in liver cancer by the cBioPortal database[19, 20] and the Catalog of Somatic Mutations in Cancer (COSMIC) database[21, 22]. The association between SGOL2 expression and immune infiltration was measured by the Tumor Immune Estimation Resource (TIMER) database[23].

2.5 Protein-protein interaction (PPI) network analysis

We used the LinkedOmics database to search for differentially expressed genes related to SGOL2 and MAD2[24] and analyzed the RNA-Seq results in the TCGA-LIHC dataset. Then, the correlation coefficients of differentially expressed genes were determined by Spearman's test. We further used the STRING database (interaction score > 0.8) and Cytoscape software (3.7.1) to construct the PPI network. We also verified the association between SGOL2 and MAD2 using GEPIA database.

2.6 Biological function and pathway enrichment analysis

We further analyzed the clusters of the network. Gene Ontology (GO) and Kyoto Encyclopedia of Genes and Genomes (KEGG) pathway analyses were then executed via the Database for Annotation, Visualization and Integrated Discovery (DAVID) and a bioinformatics online tool to determine the enriched biological processes and KEGG pathways for subsequent analysis.

2.7 Cell lines, transfection and reagents

The HCC cell lines SK-HEP-1 and HEP3B were purchased from Procell (Wuhan, China). All cells were cultured in DMEM (Gibco) supplemented with 10% fetal bovine serum (Gibco), 1% streptomycin and penicillin. Cells were transfected with lentivirus or plasmid purchased from Shanghai Genomeditech (Shanghai, China) and verified by DNA sequencing. Lentiviruses containing shNC (negative control, NC) and shSGOL2 were constructed using the vector pGMLV-SC5. The shRNA sequence used to target SGOL2 was as follows: 5'-GGTCAGAATTCCCTAACTTGT-3'. The pGMLV-SGOL2 plasmid contained the SGOL2 coding sequence. For plasmid transfection, SK-HEP-1 and HEP3B cells were seeded into 12-well plates

and then transfected with plasmids (4 mg per well) using Lipofectamine 2000 Reagent (Invitrogen) according to protocols. Cells were harvested for analysis after 48h.

2.8 Cell viability

Here, cells were seeded in 96-well plates at 2000 cells/well and incubated. Cell proliferation ability was evaluated by the cell counting kit-8 assay (CCK-8, APExBIO, USA) according to the protocol.

2.9 Apoptosis analysis and Cell cycle analysis

For cell cycle analyses, cells were fixed with 70% ethanol at 4°C overnight and stained with RNase A containing propidium iodide (Sigma-Aldrich, USA). Cell cycle distribution was determined using flow cytometry. For apoptosis analysis, cells were stained with an Annexin V-FITC/PI kit (BD Biosciences) and analyzed in a FACS Aria II flow cytometer (BD Biosciences, San Jose, USA).

2.10 Colony formation assay, Tumor sphere assay and Transwell migration and invasion assays

The colony formation assay, tumor sphere assay, migration and invasion assays of HCC cells were performed as previously described[25].

2.11 Western blot analysis and coimmunoprecipitation (WB/COIP)

Cells were seeded in 6-well plates, washed and lysed with RIPA buffer (Thermo Fisher Scientific, USA) containing protease inhibitor cocktail. SDS-PAGE and Western blotting were performed as described previously[26]. COIP was conducted as described previously using an IP/COIP kit (Absin, Shanghai, China) [27]. The following antibodies were used: secondary antibody (CST,7074/7076), GAPDH antibody (CST, 5174), SGOL2 antibody (Bethyl, A301-262A-M), MAD2 antibody (Bethyl, A300-300A), cyclin D1 antibody (CST, 55506), cyclin E1 antibody (CST, 20808), PCNA antibody (CST, 13110), normal rabbit IgG (CST, 2729), E-cadherin (CST, 14472), N-cadherin (CST, 13116), vimentin (CST, 5741), MMP9 (CST,13667), β-catenin (CST, 8480), and fibronectin (Abcam, ab268021).

2.12 Quantitative real-time PCR (qRT-PCR)

We conducted the immunohistochemistry as previously described[26]. For qRT-PCR, the following primers were used:

human SGOL2, 5'-TAAAGCACAACAACAGGGCAT-3' (forward) and

5'-AGGCGAAGAAATGTGTTCTCAAA-3' (reverse);

human MAD2, 5'-GGACTCACCTTGCTTGTAACTAC-3' (forward) and

5'-GATCACTGAACGGATTTCATCCT-3' (reverse);

2.13 Immunohistochemistry

We conducted the immunohistochemistry as previously described[26]. To detect apoptosis, samples were treated with a TUNEL BrightGreen Apoptosis Detection Kit (Vazyme, A112-03) according to the manufacturer's instructions.

2.14 Immunofluorescence assay

Cells were seeded on coverslips. The cells were fixed, permeabilized with 0.1% Triton X-100 for 1 min, blocked with 1% bovine serum albumin for 1 h, and treated with primary antibodies [SGOL2 antibody (Abcam, ab122258) and MAD2 antibody (Santa Cruz, C-10)] at 4°C overnight. The cells were then treated with secondary antibodies and incubated for 1 h and DAPI for 10 min at room temperature.

2.15 Xenograft tumor models

Male BALB/c nude mice at 6 weeks of age were purchased from the Zhejiang Academy of Medical Sciences (Hangzhou, Zhejiang). 3 Mice were subcutaneously inoculated with SK-HEP-1 shNC or SK-HEP-1 shSGOL2 cells (1×10^7 cells/200 μl serum-free DMEM). For lung metastasis model, 7 mice were intravenously injected with SK-HEP-1 shNC or SK-HEP-1 shSGOL2 cells (3×10^6 cells/200 μl serum-free DMEM) through the tail vein. The lung and liver metastasis nodules of HCC were analyzed by HE staining. Tumor volume was calculated by the following formula: tumor size = $ab^2/2$. Three weeks after inoculation, animals were euthanized, and tumors were collected and fixed for immunohistochemical analysis.

2.16 Statistical analyses

One-way ANOVA and two-tailed Student's t-tests were employed to analyze the data. All data are presented as the mean ± standard deviation (SD). We described statistical significance as follows: NS, not significant; *P ≤ 0·05; **P ≤ 0·01; ***P ≤ 0·001; ****P ≤ 0·0001. We used GraphPad Prism software version 7.0 (GraphPad Software, San Diego, CA, USA) and SPSS 20.0 software (SPSS, Chicago, IL, USA) to perform statistical analysis.

Results

3.1 | High expression of SGOL2 in HCC

We identified that SGOL2 mRNA was upregulated in various types of cancers in the Oncomine database, including hepatocellular carcinoma, colorectal cancer, lung cancer, and breast cancer (Fig. 1A). In addition, we further searched the GEPIA database to systematically assess the expression profile of SGOL2 in a variety of carcinomas (Fig. 1B). To better understand its expression levels in different diseases, including HCC, cirrhosis and dysplasia, data from the Wurmbach liver dataset were selected and further analyzed (Fig. 1C). The results showed that SGOL2 was significantly upregulated in HCC tissues compared with normal tissues ($P < 0.05$), whereas there was no significant difference between the cirrhosis, dysplasia and normal liver tissue groups. Moreover, SGOL2 protein expression was analyzed

using the HPA database. As shown in Fig. 1D, SGOL2 was not detected in the normal liver (Patient ID: 3402) and showed weak staining in the HCC liver (Patient IDs: 2429/2279). Furthermore, we analyzed the protein levels of SGOL2 in HCC and matched adjacent normal tissues of patients in cohort 2 by Western blot and found that SGOL2 was significantly upregulated in HCC (Fig. 1E), and immunohistochemistry (IHC) staining from the two independent HCC cohorts confirmed the results (Fig. 1F-H). In addition, we divided the patients in cohort 2 into 2 groups according to differentiation levels: a well-differentiated group and a poorly differentiated group. Interestingly, the expression levels of SGOL2 in the poorly differentiated group were significantly higher than those in the well-differentiated group, indicating that the expression level of SGOL2 is directly proportional to tumor progression (Fig. 1H). Similarly, we found the same result: the expression level of SGOL2 in the Grade 3 group was significantly higher than that in the Grade 1/2 group in cohort 1 (supplement Table 1, p = 0.001).

To expand the number of patients included in the analysis, we further confirmed the overexpression of SGOL2 in HCC data from TCGA. We found that the expression level of SGOL2 showed a positive association with grade levels (Fig. 2G), consistent with our previous results in cohorts 1 and 2. Moreover, SGOL2 was found to be roughly proportional to stage levels (Fig. 2B). As shown in Fig. 2A, SGOL2 mRNA levels were higher in HCC samples (n = 371) than in normal samples (n = 50). We also conducted subgroup analysis in various subgroups (race, sex, age, weight), which showed significantly elevated SGOL2 expression levels (Fig. 2C-F). In addition, SGOL2 was significantly elevated in TP53-mutant patients (Fig. 2I). Interestingly, there was no significant difference between HCC patients with and without lymph node metastasis (Fig. 2H). Thus, these results indicated that the SGOL2 overexpression was related the development of HCC.

3.2 | Upregulation of SGOL2 indicated poor prognosis in HCC patients

To identify whether SGOL2 could be a novel prognostic marker in HCC, we used the Kaplan-Meier Plotter database to analyze its prognostic significance in HCC patients. SGOL2 overexpression was closely related to poor overall survival (OS, HR = 2.29 (1.6–3.28), P = 3.5e-06), relapse-free survival (RFS, HR = 1.96 (1.38–2.78), P = 0.00013), progression-free survival (PFS, HR = 2.1 (1.55–2.84), P = 9.2e-07) and disease-specific survival (DSS, HR = 2.84 (1.81–4.47), P = 2.3e-06) in HCC patients (Fig. 3A-D). To better identify the negative correlation between the expression level of SGOL2 and the prognosis of liver cancer, we performed survival analysis in verification cohort 1. According to the immunohistochemical score, we divided the patients (n = 97) in cohort 1 into a low expression group (n = 44) and a high expression group (n = 53) and then performed survival analysis. As shown in Fig. 3E, we found that the overall survival (OS) of the high expression group was significantly lower than that of the low expression group (p = 0.001). Subsequently, we conducted a SGOL2-based prognostic model. All HCC patients in cohort 1 were randomly divided into two groups: training group (n = 67), validation group (n = 30). Next, we identified four variables which were closely related to survival: expression, grade, AJCC TNM and AFP based on lasso regression model (Fig. 3F, G). We also established a nomogram to predict the 3-year survival of HCC patients based on the multivariable Cox proportional hazards model (Fig. 3H), whose discrimination power was evaluated by receiver operating characteristic (ROC) curves. The areas under the ROC curve

(AUCs) of the 3-year survival probability in the training and validation groups were 0.898 and 0.687, respectively (Fig. 3I-K). The calibration curves of the nomogram showed good probability consistencies between the prediction and observation (Fig. 3L,M). In conclusion, high SGOL2 expression was associated with poor prognosis in HCC patients.

3.3 | The association between SGOL2 expression and immune infiltration, mutations in HCC

Next, we assessed the mutation frequency of SGOL2 in HCC. The somatic mutation frequency of SGOL2 in HCC was 0.7% (Fig. 4A). Thus, we further evaluated the mutation types of SGOL2 in COSMIC. As shown in Fig. 4B, 45.80% of the samples showed missense substitutions, and 13.19% of the samples showed synonymous substitutions. As shown in Fig. 4C, the substitution mutations mainly occurred at C > T (74 samples, 17.96%). Then, we used the TIMER database to identify the association between SGOL2 expression and immune infiltration. We evaluated the relationship between SGOL2 expression and immune cells abundances. As shown in Fig. 4D, SGOL2 expression had a slightly positive correlation with tumor purity (Cor = 0.148, P = 5.68E-03). Moreover, SGOL2 expression had dramatically positive correlations with all immune infiltrates, especially macrophages (Cor = 0.483, P = 2.69E-21) and dendritic cells (Cor = 0.47, P = 3.99E-20).

3.4 | SGOL2 promoted malignancy of HCC cells in vitro and in vivo

SK-HEP-1 and HEP3B cells were chosen to evaluate the function of SGOL2 according to the mRNA levels of SGOL2 in different HCC cell lines based on the data from CCLE (Fig. 5A). After transfection with lentivirus, we confirmed that SGOL2 was significantly decreased at both the mRNA and protein levels by RT-PCR and Western blot, respectively (Fig. 5B, C). Transwell assays indicated that low SGOL2 expression suppressed the migration and invasion of HCC cells (Fig. 5D, E). Moreover, we also tested the expression alterations of key EMT-related proteins responding to the downregulation of SGOL2 (Fig. 5K). Interestingly, the results showed that shSGOL2 resulted in increased expression of E-cadherin and reduced expression of N-cadherin, fibronectin, vimentin, β-catenin, and MMP9. Thus, downregulation of SGOL2 could inhibit cell metastasis by repressing migration, invasion and EMT in HCC. Next, a sphere formation assay was performed to determine whether stemness could be influenced by downregulating SGOL2. Consistently, the spheres in the shSGOL2 group were dramatically fewer and smaller than those in the shNC group (Fig. 5F). Furthermore, the shSGOL2 group developed fewer cell colonies than the NC group (Fig. 5G), and we also observed that low SGOL2 expression suppressed the proliferation of HCC cells by CCK-8 assay (Fig. 5J). In addition, flow cytometry-based assays demonstrated that apoptotic indices in the shSGOL2 group were dramatically higher than those in the NC group (Fig. 5H), and the cell cycle was strongly influenced by the downregulation of SGOL2 (Fig. 5I). To further verify the role of SGOL2 in HCC in vivo, xenograft tumor models were constructed by SK-HEP-1 shNC and SK-HEP-1 shSGOL2. The mice were sacrificed on day 21 after inoculation, and the formed tumors, lung and liver were statistically analyzed (Fig. 6A, B). Both the volumes and weights of the formed tumors were dramatically decreased in the shSGOL2 group compared with the shNC group (Fig. 6B). We further analyzed angiogenesis markers (CD34), proliferation markers (Ki-67 and proliferating cell nuclear antigen

[PCNA]), and EMT-related markers (E-cadherin, N-cadherin, vimentin, Snail, and Slug) in xenograft specimens by IHC. Downregulation of SGOL2 led to a reduction in proliferation and metastasis (Fig. 6C, D), which was consistent with the above in vitro results. We also found that the apoptotic area in the shSGOL2 group was much larger than that in the shNC group (Fig. 6E). Thus, these data indicated that SGOL2 promoted tumor growth and metastasis in vitro and in vivo.

3.5 | MAD2 overexpression was closely related to SGOL2 and indicated poor prognosis in HCC patients

Next, we tried to clarify the signal transduction pathway of SGOL2 in HCC cells. SGOL2 and MAD2 were reported to be involved in the separation of eukaryotic sister chromatids during the cell cycle[28]. Thus, we hypothesized that SGOL2 promotes tumors by influencing the expression of MAD2. To explore the role of MAD2 in liver cancer, a factor closely related to SGOL2, we evaluated its expression and prognostic significance by the UALCAN database. As shown in Fig. 7A, MAD2 was also markedly upregulated in HCC. Moreover, we found that the expression of MAD2 in HCC was positively correlated with SGOL2 in the TCGA database (R = 0.78, P = 0) (Fig. 7B). Interestingly, we found that high MAD2 expression was also related to poor OS, RFS and PFS in HCC patients (Fig. 7C-E).

3.6 | Differentially expressed genes associated with SGOL2 and MAD2 in HCC

We used the data from the LinkedOmics database for analysis to identify differential genes related to both SGOL2 and MAD2 in HCC by Spearman's test (Fig. 8A, D). The top 50 positively and top 50 negatively correlated markers were represented in Fig. 8B-F. Then, the positively correlated genes with coefficients > 0.8 were selected for further analysis. In total, we identified 85 genes positively associated with SGOL2 and 51 genes positively related to MAD2. Among these, we identified 47 genes positively related to both SGOL2 and MAD2 (Fig. 9A). Then, we constructed a PPI network based on the 47 differentially expressed genes using STRING and Cytoscape (Fig. 9B) and used it for GO and KEGG enrichment analysis (Fig. 9C-F).

3.7 | Identify hub genes and their prognostic significance in HCC

The top 15 hub genes of the network were chosen for further analysis using cytoHubba based on the clusters identified in the PPI network using MCODE (Fig. 10A). Biological processes, such as cell division, cell proliferation and apoptotic process, were significantly affected and enriched based on GO analysis results (Fig. 10B). The coexpressed genes were mainly involved in the cell cycle, progesterone-mediated oocyte maturation, oocyte meiosis and p53 signaling pathway based on KEGG results (Fig. 10C). Then, we tried to assess whether these identified hub genes were related to prognosis or not. All 15 genes were significantly related to poor OS (BUB1B, NUSAP1, TTK, CCNB2, TOP2A, KIF2C, CCNB1, KIF23, TPX2, KIF11, KIF4A, CDK1, BUB1, CENPE, CDCA8) (Fig. 10D).

3.8 | SGOL2 dysregulated the cell cycle process by activating the MAD2 protein

To validate these data through the bioinformatics analysis above, we further demonstrated the role of SGOL2 in HCC cells, especially in cell cycle process based on above results. First, we found that the protein level of MAD2 was extremely decreased in HCC cells through downregulating SGOL2 (Fig. 11A), while overexpression of SGOL2 increased the expression of MAD2 (Fig. 11B). After knockdown of SGOL2, the protein levels of PCNA, cyclin D1 and cyclin E1 were significantly decreased (Fig. 11A), whereas upregulation of SGOL2 extremely increased the expression of PCNA, cyclin D1 and cyclin E1 (Fig. 11B). Furthermore, when MAD2 was blocked by its specific inhibitor M2I-1, highly aggressive malignant behaviors of HCC cells caused by overexpression of SGOL2 were significantly reversed (Fig. 11C, D). Altogether, these data indicated that SGOL2 dysregulated the cell cycle and promoted the development of HCC by activating the MAD2 protein.

3.9 | SGOL2 exerted its effect by directly binding with MAD2

Next, we were interested in defining whether SGOL2 could directly interact with MAD2. Immunofluorescence (IF) staining showed that SGOL2 colocalized with MAD2 in both SK-HEP-1 and HEP3B cell lines (Fig. 12A), and the coimmunoprecipitation (Co-IP) assay further verified that SGOL2 could bind with MAD2 (Fig. 12B). Altogether, these data collectively verified that SGOL2, binding with MAD2 and forming a SGOL2-MAD2 complex, activated MAD2 and then fueled tumor cell growth by dysregulating the cell cycle process, which finally promoted the malignant behaviors of HCC cells, including proliferation, migration, invasion, stemness and EMT (Fig. 12C).

Discussion

The accurate separation of duplicated genomes in mitosis is fundamental for cells[29]. Chromosome segregation errors can lead to chromosomal instability (CIN), which induces tumorigenesis[30–34]. CIN could also lead to the diversity in somatic copy number alterations (SCNAs), potentially providing the fundamental basis for tumor development and progression[29, 35–37]. SGOL2 is fundamental to separating sister chromatids[9]. A previous study revealed that SGOL2 together with MAD2 was closely related to the spindle assembly checkpoint (SAC)[16]. HCC is characterized by dysfunctional cell cycle progression and uncontrolled rapid proliferation[38, 39]. However, it is not clear whether SGOL2 has any role in HCC and how it works. In this study, we analyzed the role of SGOL2 in HCC and demonstrated that its overexpression promoted the development and progression of HCC, while its deficiency suppressed tumorigenesis. It was further validated that SGOL2 acted as an oncogene by directly regulating MAD2 and then dysregulated the cell cycle process in HCC.

MAD2 is a key protein in the spindle assembly checkpoint (SAC), encoded by an 11.5 kbp gene on chromosome 4q27[40, 41]. It has been reported that MAD2 is overexpressed and correlated with cancer progression in different types of cancers, including colon, pancreatic, liver and lung cancers[42]. Moreover, MAD2-overexpressing patients may benefit from MAD2-targeted therapy, which could dramatically dysregulate the cell cycle, effectively activate apoptosis and weaken the proliferation, metastasis and

stemness of tumor cells[43–47]. It was also reported that knock-down of MAD2 induced apoptotic signal transduction and added the sensitivity of lung cancer cells to cisplatin[43]. Thus, targeting MAD2 is well recognized as an efficient cancer manipulation strategy. According to a report[28], SGOL2 combined with MAD2 is involved in the regulation of the cell cycle process. In addition, we found that the cell cycle may be regulated by SGOL2 and MAD2 based on protein-protein interaction (PPI) network analysis and pathway enrichment analysis. Therefore, we assumed that MAD2 may be the downstream target of SGOL2, and we further conducted loss-of-function and rescue tests. We found that loss of SGOL2 significantly suppressed the expression of MAD2 and markers related to the cell cycle. Furthermore, the promoting effect of upregulated SGOL2 on the malignant behaviors of HCC cells was dramatically reversed by the addition of the MAD2-specific inhibitor M2I-1. Cyclin D1 and cyclin E1, as vital regulatory markers of G1/S phase cell cycle phase, are related to the development of various cancers[48–51]. Therefore, we concluded that SGOL2 downregulation inhibited the expression of MAD2, thereby reducing the levels of cyclin D1 and cyclin E1, inducing cell cycle arrest in G1/S phase, and inhibiting the proliferation of HCC cells.

The regulation of MAD2 by SGOL2 has been investigated, and we are further interested in clarifying the molecular mechanism. As reported, SGOL2-MAD2 functions by manipulating the separation of eukaryotic sister chromatids during the cell cycle[28]. Intriguingly, we found that MAD2 expression showed a positive correlation with SGOL2. Immunofluorescence assays showed that SGOL2 colocalized with MAD2, which was further validated by a Co-IP assay. This finding indicated that SGOL2 and MAD2 were closely linked and may function together. In previous studies, MAD2 formed the MAD2-CDC20 complex and further combined with Mad3 (BubR1) and Bub3 to form the mitotic checkpoint complex that inhibits APC/C[52, 53]. Another report showed that closed MAD2 bound to MAD1, forming a MAD1/MAD2 complex, represented a template for MAD2 bound to CDC20 in the spindle assembly checkpoint[40]. In this study, our data demonstrated that SGOL2, which binds with MAD2, activates MAD2 and further promotes tumor growth in HCC.

As a member of the shugoshin family, there are fewer reports of how SGOL2 works in cancer than SGOL1, which has been repeatedly demonstrated to be associated with the occurrence and development of cancers[54–62]. It was reported that elevated expression of SGOL2 related to the abundance of tumor-infiltrating mast cells (TIMCs) indicated poor prognosis in adrenocortical carcinoma[63]. In this study, SGOL2 mainly exerted its tumor-promoting effects by activating MAD2 and then dysregulating the cell cycle in HCC. We first proved that SGOL2 directly activates MAD2 in HCC cells, which indicates that it may serve as a potential target for molecular-based therapy.

Nevertheless, there are several limitations to this study. First, some of the in vitro results may need to be further validated in vivo. Secondly, we should also pay attention to the alterations of other pathways regulated by SGOL2 in addition to manipulating the cell cycle.

Conclusions

Taken together, these results suggest that SGOL2 is a novel functional oncogene in HCC and that it accelerates tumor growth by regulating the cell cycle via the activation of MAD2. Moreover, SGOL2 is a potential target and clinical marker for HCC therapy. The role of SGOL2 in promoting tumorigenesis in HCC is reported here for the first time, indicating that a novel therapeutic strategy for HCC involving SGOL2 is worthy of further investigation.

Abbreviations

HCC: Hepatocellular carcinoma

SGOL2: Shugoshin-like protein 2

MAD2: mitotic arrest deficient 2 like 1

PP2A: protein phosphatase 2 A

IHC: immunohistochemistry

LIC: liver hepatocellular carcinoma

OS: overall survival (OS)

RFS: relapse-free survival (RFS)

PFS: progression-free survival (PFS)

DSS: disease-specific survival (DSS)

TCGA: The Cancer Genome Atlas

CCK8: Cell counting kit 8

WB: western blot

COIP: coimmunoprecipitation

qRT-PCR: quantitative real-time PCR

PCNA: proliferating cell nuclear antigen

IF: immunofluorescence

CIN: chromosomal instability

SAC: spindle assembly checkpoint

TIMCs: tumor-infiltrating mast cells

GEPIA: Gene Expression Profiling Interactive Analysis

HPA: Human Protein Atlas

COSMIC: Catalog of Somatic Mutations in Cancer

TIMER: Tumor Immune Estimation Resource

GO: Gene Ontology

KEGG: Kyoto Encyclopedia of Genes and Genomes

DAVID: Database for Annotation, Visualization and Integrated Discovery

PPI: protein-protein interaction

Declarations

Ethics approval and consent to participate

This study was approved by the Research Ethics Committee of Zhejiang University. All experiments were performed according to the relevant regulations.

Consent for publication

All materials and images are original. No consent needs to declare.

Availability of data and material

Data, materials and software information supporting the conclusions of this article are included within the article and its additional file.

Competing interests

The authors have declared no conflicts of interest.

Funding

This study was supported by Key research and development project of Department of Science and Technology of Zhejiang Province (2017C03051), Science Fund for Creative Research Groups of the National Natural Science Foundation of China (No.81721091) and A Project Supported by Scientific Research Fund of Zhejiang Provincial Education Department (Y202045600).

Authors' Contributions

LLJ designed the study. HQQ, HXC and ZYL supervised data collection and data management. ZLJ and YY help with animal experiments. HQQ and HXC analyzed the data. HQQ prepared the first draft of the manuscript. All authors wrote the paper, had access to the study data, and have reviewed and approved the final manuscript.

Acknowledgements

We thank all the participants who contributed to our work.

Authors' information

State Key Laboratory for Diagnosis and Treatment of Infectious Diseases, National Clinical Research Center for Infectious Diseases, Collaborative Innovation Center for Diagnosis and Treatment of Infectious Diseases, The First Affiliated Hospital, College of Medicine, Zhejiang University, Hangzhou, China.

Qingqing Hu, Yalei Zhao, Lingjian Zhang, Ya Yang, Lanjuan Li

Department of Oncology, The Affiliated Huai'an No.1 People's Hospital, Nanjing Medical University, Huai'an, China.

Xiaochu Hu

References

1. Forner A, Reig M, Bruix J. Hepatocellular carcinoma. Lancet (London, England). 2018;391(10127):1301-14.
2. Kudo M. Recent Advances in Systemic Therapy for Hepatocellular Carcinoma in an Aging Society: 2020 Update. Liver cancer. 2020;9(6):640-62.
3. Novikova MV, Khromova NV, Kopnin PB. Components of the Hepatocellular Carcinoma Microenvironment and Their Role in Tumor Progression. Biochemistry Biokhimiia. 2017;82(8):861-73.
4. Barbero JL. Sister chromatid cohesion control and aneuploidy. Cytogenetic and genome research. 2011;133(2-4):223-33.
5. Tucker JD, Preston RJ. Chromosome aberrations, micronuclei, aneuploidy, sister chromatid exchanges, and cancer risk assessment. Mutation research. 1996;365(1-3):147-59.
6. Solomon DA, Kim T, Diaz-Martinez LA, et al. Mutational inactivation of STAG2 causes aneuploidy in human cancer. Science (New York, NY). 2011;333(6045):1039-43.
7. Kitajima TS, Kawashima SA, Watanabe Y. The conserved kinetochore protein shugoshin protects centromeric cohesion during meiosis. Nature. 2004;427(6974):510-7.
8. Tanno Y, Susumu H, Kawamura M, Sugimura H, Honda T, Watanabe Y. The inner centromere-shugoshin network prevents chromosomal instability. Science (New York, NY). 2015;349(6253):1237-40.

9. Gutiérrez-Caballero C, Cebollero LR, Pendás AM. Shugoshins: from protectors of cohesion to versatile adaptors at the centromere. Trends in genetics : TIG. 2012;28(7):351-60.
10. Kitajima TS, Sakuno T, Ishiguro K, et al. Shugoshin collaborates with protein phosphatase 2A to protect cohesin. Nature. 2006;441(7089):46-52.
11. Marston AL. Shugoshins: tension-sensitive pericentromeric adaptors safeguarding chromosome segregation. Molecular and cellular biology. 2015;35(4):634-48.
12. Riedel CG, Katis VL, Katou Y, et al. Protein phosphatase 2A protects centromeric sister chromatid cohesion during meiosis I. Nature. 2006;441(7089):53-61.
13. Watanabe Y, Kitajima TS. Shugoshin protects cohesin complexes at centromeres. Philosophical transactions of the Royal Society of London Series B, Biological sciences. 2005;360(1455):515-21, discussion 21.
14. Watanabe Y. Shugoshin: guardian spirit at the centromere. Current opinion in cell biology. 2005;17(6):590-5.
15. Tashiro S, Handa T, Matsuda A, et al. Shugoshin forms a specialized chromatin domain at subtelomeres that regulates transcription and replication timing. Nat Commun. 2016;7:10393.
16. Orth M, Mayer B, Rehm K, et al. Shugoshin is a Mad1/Cdc20-like interactor of Mad2. The EMBO journal. 2011;30(14):2868-80.
17. Faridi R, Rehman AU, Morell RJ, et al. Mutations of SGO2 and CLDN14 collectively cause coincidental Perrault syndrome. Clinical genetics. 2017;91(2):328-32.
18. Gantchev J, Martínez Villarreal A, Xie P, et al. The Ectopic Expression of Meiosis Regulatory Genes in Cutaneous T-Cell Lymphomas (CTCL). Frontiers in oncology. 2019;9:429.
19. Cerami E, Gao J, Dogrusoz U, et al. The cBio cancer genomics portal: an open platform for exploring multidimensional cancer genomics data. Cancer discovery. 2012;2(5):401-4.
20. Gao J, Aksoy BA, Dogrusoz U, et al. Integrative analysis of complex cancer genomics and clinical profiles using the cBioPortal. Science signaling. 2013;6(269):pl1.
21. Forbes SA, Beare D, Gunasekaran P, et al. COSMIC: exploring the world's knowledge of somatic mutations in human cancer. Nucleic acids research. 2015;43(Database issue):D805-11.
22. Forbes SA, Beare D, Boutselakis H, et al. COSMIC: somatic cancer genetics at high-resolution. Nucleic acids research. 2017;45(D1):D777-d83.
23. Li T, Fan J, Wang B, et al. TIMER: A Web Server for Comprehensive Analysis of Tumor-Infiltrating Immune Cells. Cancer research. 2017;77(21):e108-e10.
24. Vasaikar SV, Straub P, Wang J, Zhang B. LinkedOmics: analyzing multi-omics data within and across 32 cancer types. Nucleic acids research. 2018;46(D1):D956-d63.
25. Hu Q, Hu X, Zhang L, Zhao Y, Li L. Targeting Hedgehog signalling in CD133-positive hepatocellular carcinoma: improving Lenvatinib therapeutic efficiency. Medical Oncology. 2021;38(4):41.
26. Qian F, Hu Q, Tian Y, et al. ING4 suppresses hepatocellular carcinoma via a NF-κB/miR-155/FOXO3a signaling axis. International journal of biological sciences. 2019;15(2):369-85.

27. Zhao Y, Xue C, Xie Z, Ouyang X, Li L. Comprehensive analysis of ubiquitin-specific protease 1 reveals its importance in hepatocellular carcinoma. Cell Prolif. 2020;53(10):e12908.
28. Hellmuth S, Gomez HL, Pendas AM, Stemmann O. Securin-independent regulation of separase by checkpoint-induced shugoshin-MAD2. Nature. 2020;580(7804):536-41.
29. Zack TI, Schumacher SE, Carter SL, et al. Pan-cancer patterns of somatic copy number alteration. Nature genetics. 2013;45(10):1134-40.
30. Carter SL, Eklund AC, Kohane IS, Harris LN, Szallasi Z. A signature of chromosomal instability inferred from gene expression profiles predicts clinical outcome in multiple human cancers. Nature genetics. 2006;38(9):1043-8.
31. Hieronymus H, Murali R, Tin A, et al. Tumor copy number alteration burden is a pan-cancer prognostic factor associated with recurrence and death. Elife. 2018;7:e37294. Published 2018 Sep 4. doi:10.7554/eLife.37294
32. Jamal-Hanjani M, Wilson GA, McGranahan N, et al. Tracking the Evolution of Non-Small-Cell Lung Cancer. N Engl J Med. 2017;376(22):2109-21.
33. McGranahan N, Burrell RA, Endesfelder D, Novelli MR, Swanton C. Cancer chromosomal instability: therapeutic and diagnostic challenges. EMBO reports. 2012;13(6):528-38.
34. Schwarz RF, Ng CK, Cooke SL, et al. Spatial and temporal heterogeneity in high-grade serous ovarian cancer: a phylogenetic analysis. PLoS medicine. 2015;12(2):e1001789.
35. Davoli T, Xu AW, Mengwasser KE, et al. Cumulative haploinsufficiency and triplosensitivity drive aneuploidy patterns and shape the cancer genome. Cell. 2013;155(4):948-62.
36. Turajlic S, Xu H, Litchfield K, et al. Deterministic Evolutionary Trajectories Influence Primary Tumor Growth: TRACERx Renal. Cell. 2018;173(3):595-610.e11.
37. Watkins TBK, Lim EL, Petkovic M, et al. Pervasive chromosomal instability and karyotype order in tumour evolution. Nature. 2020;587(7832):126-32.
38. Hikita H, Takehara T, Shimizu S, et al. The Bcl-xL inhibitor, ABT-737, efficiently induces apoptosis and suppresses growth of hepatoma cells in combination with sorafenib. Hepatology. 2010;52(4):1310-21.
39. Wang C, Cigliano A, Delogu S, et al. Functional crosstalk between AKT/mTOR and Ras/MAPK pathways in hepatocarcinogenesis: implications for the treatment of human liver cancer. Cell cycle (Georgetown, Tex). 2013;12(13):1999-2010.
40. De Antoni A, Pearson CG, Cimini D, et al. The Mad1/Mad2 Complex as a Template for Mad2 Activation in the Spindle Assembly Checkpoint. Current Biology. 2005;15(3):214-25.
41. Rosenberg SC, Corbett KD. The multifaceted roles of the HORMA domain in cellular signaling. Journal of Cell Biology. 2015;211(4):745-55.
42. Byrne T, Coleman HG, Cooper JA, McCluggage WG, McCann A, Furlong F. The association between MAD2 and prognosis in cancer: a systematic review and meta-analyses. Oncotarget; Vol 8, No 60. 2017.

43. Nascimento AV, Singh A, Bousbaa H, Ferreira D, Sarmento B, Amiji MM. Overcoming cisplatin resistance in non-small cell lung cancer with Mad2 silencing siRNA delivered systemically using EGFR-targeted chitosan nanoparticles. Acta Biomaterialia. 2017;47:71-80.
44. Yu L, Guo W, Zhao S, Tang J, Liu J. Knockdown of Mad2 induces osteosarcoma cell apoptosis-involved Rad21 cleavage. Journal of Orthopaedic Science. 2011;16(6):814-20.
45. Pajuelo-Lozano N, Alcala S, Sainz B, Jr., Perona R, Sanchez-Perez I. Targeting MAD2 modulates stemness and tumorigenesis in human Gastric Cancer cell lines. Theranostics. 2020;10(21):9601-18.
46. Sotillo R, Hernando E, Díaz-Rodríguez E, et al. Mad2 Overexpression Promotes Aneuploidy and Tumorigenesis in Mice. Cancer Cell. 2007;11(1):9-23.
47. Li Y, Bai W, Zhang J. MiR-200c-5p suppresses proliferation and metastasis of human hepatocellular carcinoma (HCC) via suppressing MAD2L1. Biomed Pharmacother. 2017;92:1038-44.
48. Alao JP. The regulation of cyclin D1 degradation: roles in cancer development and the potential for therapeutic invention. Mol Cancer. 2007;6:24.
49. Masamha CP, Benbrook DM. Cyclin D1 degradation is sufficient to induce G1 cell cycle arrest despite constitutive expression of cyclin E2 in ovarian cancer cells. Cancer research. 2009;69(16):6565-72.
50. Möröy T, Geisen C. Cyclin E. The international journal of biochemistry & cell biology. 2004;36(8):1424-39.
51. Yu XJ, Han QB, Wen ZS, Ma L, Gao J, Zhou GB. Gambogenic acid induces G1 arrest via GSK3β-dependent cyclin D1 degradation and triggers autophagy in lung cancer cells. Cancer Lett. 2012;322(2):185-94.
52. Corbett KD. Molecular Mechanisms of Spindle Assembly Checkpoint Activation and Silencing. Progress in molecular and subcellular biology. 2017;56:429-55.
53. Lara-Gonzalez P, Kim T, Oegema K, Corbett K, Desai A. A tripartite mechanism catalyzes Mad2-Cdc20 assembly at unattached kinetochores. Science (New York, NY). 2021;371(6524):64-7.
54. Sun W, He B, Yang B, et al. Genome-wide CRISPR screen reveals SGOL1 as a druggable target of sorafenib-treated hepatocellular carcinoma. Laboratory investigation; a journal of technical methods and pathology. 2018;98(6):734-44.
55. Chen Q, Wan X, Chen Y, Liu C, Gu M, Wang Z. SGO1 induces proliferation and metastasis of prostate cancer through AKT-mediated signaling pathway. Am J Cancer Res. 2019 Dec 1;9(12):2693-2705. PMID: 31911855; PMCID: PMC6943359.
56. Matsuura S, Kahyo T, Shinmura K, et al. SGOL1 variant B induces abnormal mitosis and resistance to taxane in non-small cell lung cancers. Scientific reports. 2013;3:3012.
57. Nasim N, Ghafouri-Fard S, Soleimani S, et al. Assessment of SGO1 and SGO1-AS1 contribution in breast cancer. Human antibodies. 2019;27(4):279-84.
58. Rao CV, Sanghera S, Zhang Y, et al. Systemic Chromosome Instability Resulted in Colonic Transcriptomic Changes in Metabolic, Proliferation, and Stem Cell Regulators in Sgo1-/+ Mice. Cancer research. 2016;76(3):630-42.

59. Wang LH, Yen CJ, Li TN, Elowe S, Wang WC, Wang LH. Sgo1 is a potential therapeutic target for hepatocellular carcinoma. Oncotarget. 2015;6(4):2023-33.
60. Wang Y, Liu L, Liu X, et al. Shugoshin1 enhances multidrug resistance of gastric cancer cells by regulating MRP1, Bcl-2, and Bax genes. Tumour biology : the journal of the International Society for Oncodevelopmental Biology and Medicine. 2013;34(4):2205-14.
61. Yang J, Ikezoe T, Nishioka C, Yokoyama A. A novel treatment strategy targeting shugoshin 1 in hematological malignancies. Leukemia research. 2013;37(1):76-82.
62. Zhang Q, Liu H. Functioning mechanisms of Shugoshin-1 in centromeric cohesion during mitosis. Essays in biochemistry. 2020;64(2):289-97.
63. Tian X, Xu W, Wang Y, et al. Identification of tumor-infiltrating immune cells and prognostic validation of tumor-infiltrating mast cells in adrenocortical carcinoma: results from bioinformatics and real-world data. Oncoimmunology. 2020;9(1):1784529.

Figures

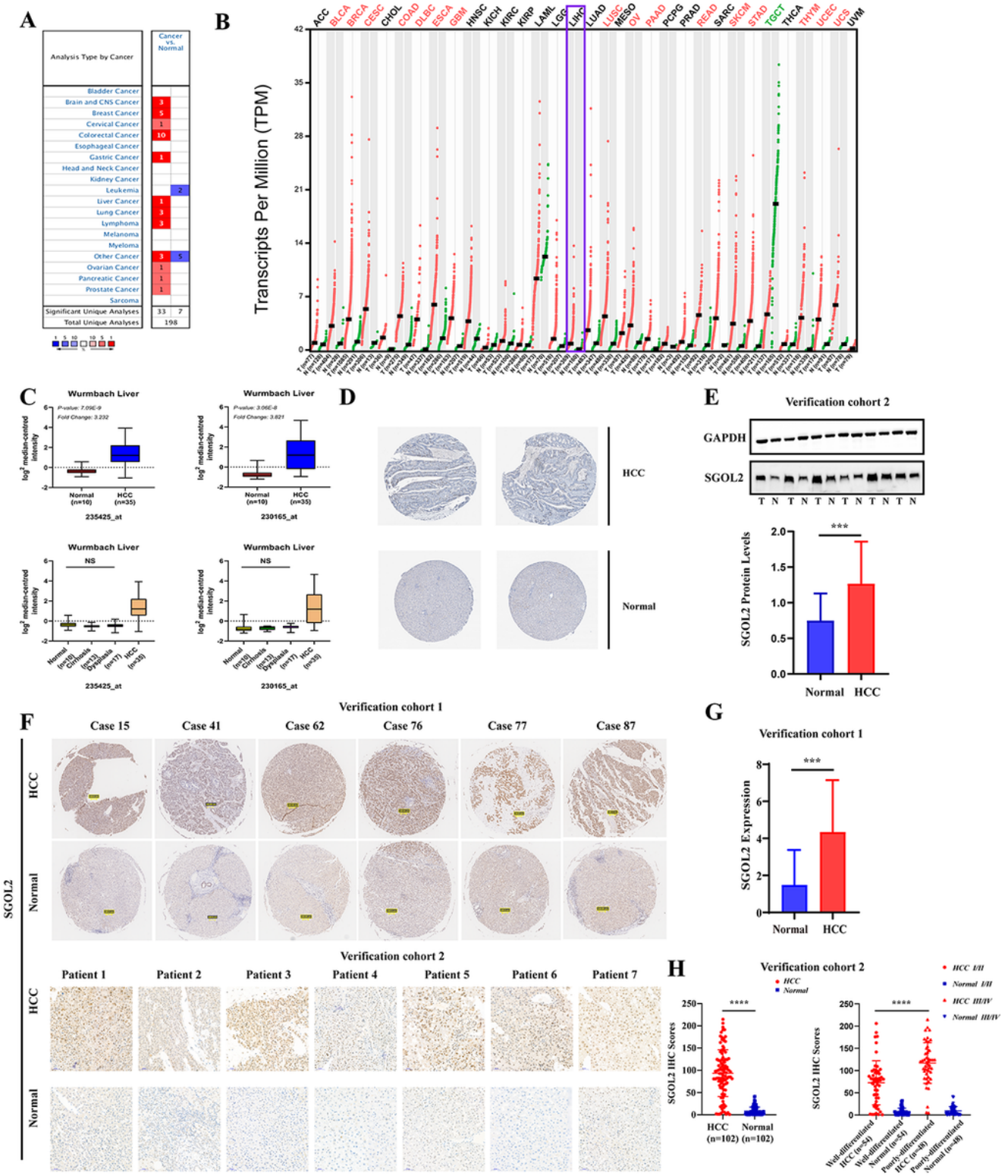

Figure 1

The elevated expression of SGOL2 in hepatocellular carcinoma (HCC). A-B, SGOL2 overexpression were detected in various types of cancers (Oncomine database and GEPIA database). C, SGOL2 is overexpressed in hepatocellular carcinoma (HCC) (Oncomine database, Wurmbach liver). D-G, Protein expression of SGOL2 is elevated in HCC patients (HPA database and cohort 1/2). H, Protein expression of

SGOL2 in poorly differentiated group was significantly higher than that in well-differentiated group of cohort 2. Results are presented as mean ± SD, *P<0.05, **P<0.01, ***P<0.001, ****P<0.0001.

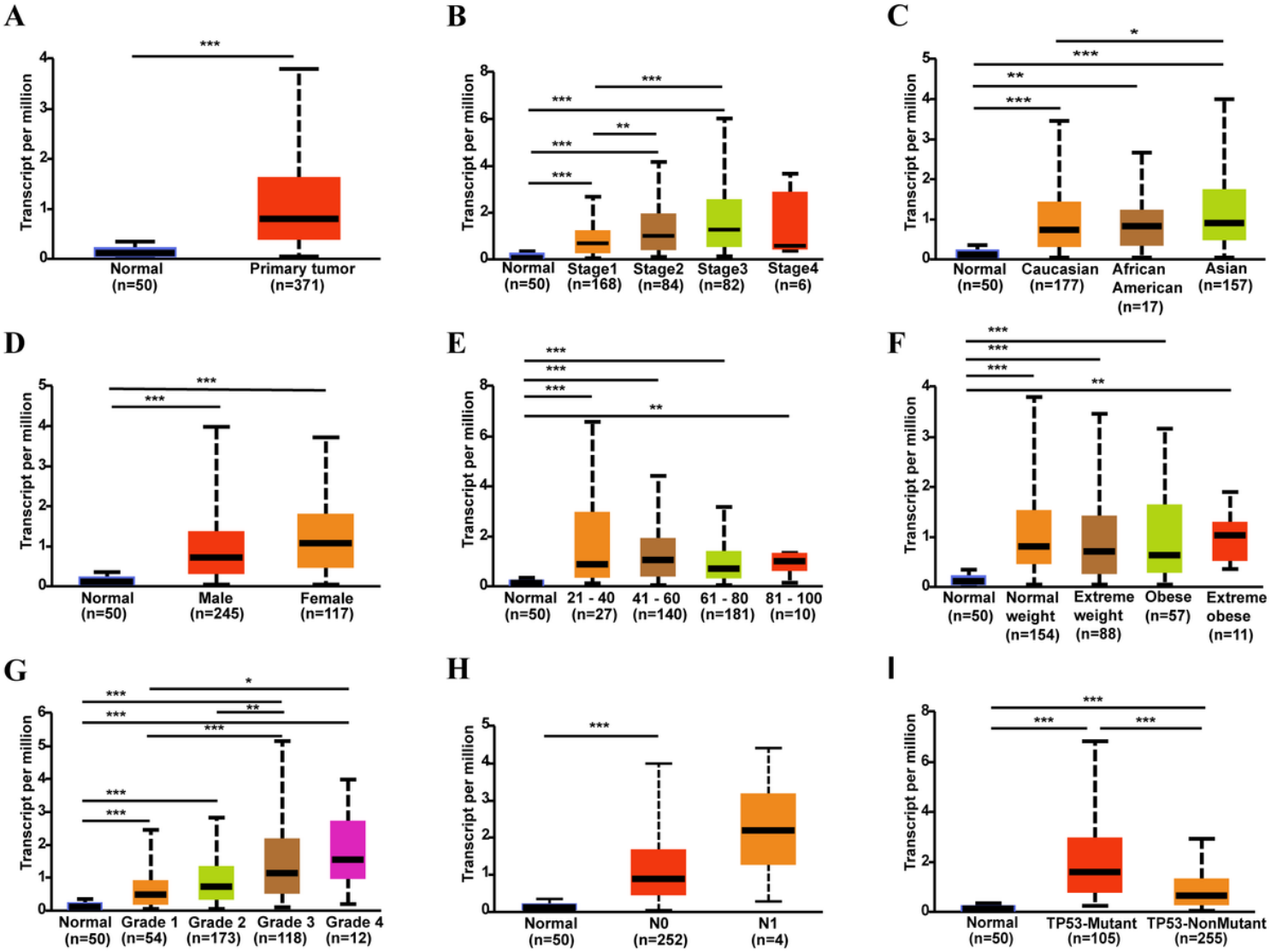

Figure 2

Subgroup expression analysis of SGOL2 in HCC. A, mRNA expression of SGOL2 in normal and HCC patients. B, SGOL2 mRNA expression levels of HCC patients with different tumor stages. C-F, SGOL2 mRNA expression levels of HCC patients in subgroups with different races, genders, ages and weights. G, SGOL2 mRNA expression levels of HCC patients with different tumor grades. H, SGOL2 mRNA expression levels of HCC patients with different metastasis status. I SGOL2 mRNA expression levels of HCC patients with TP-53 mutant or TP-53 non-mutant. *P<0.05, **P<0.01, ***P<0.001, ****P<0.0001.

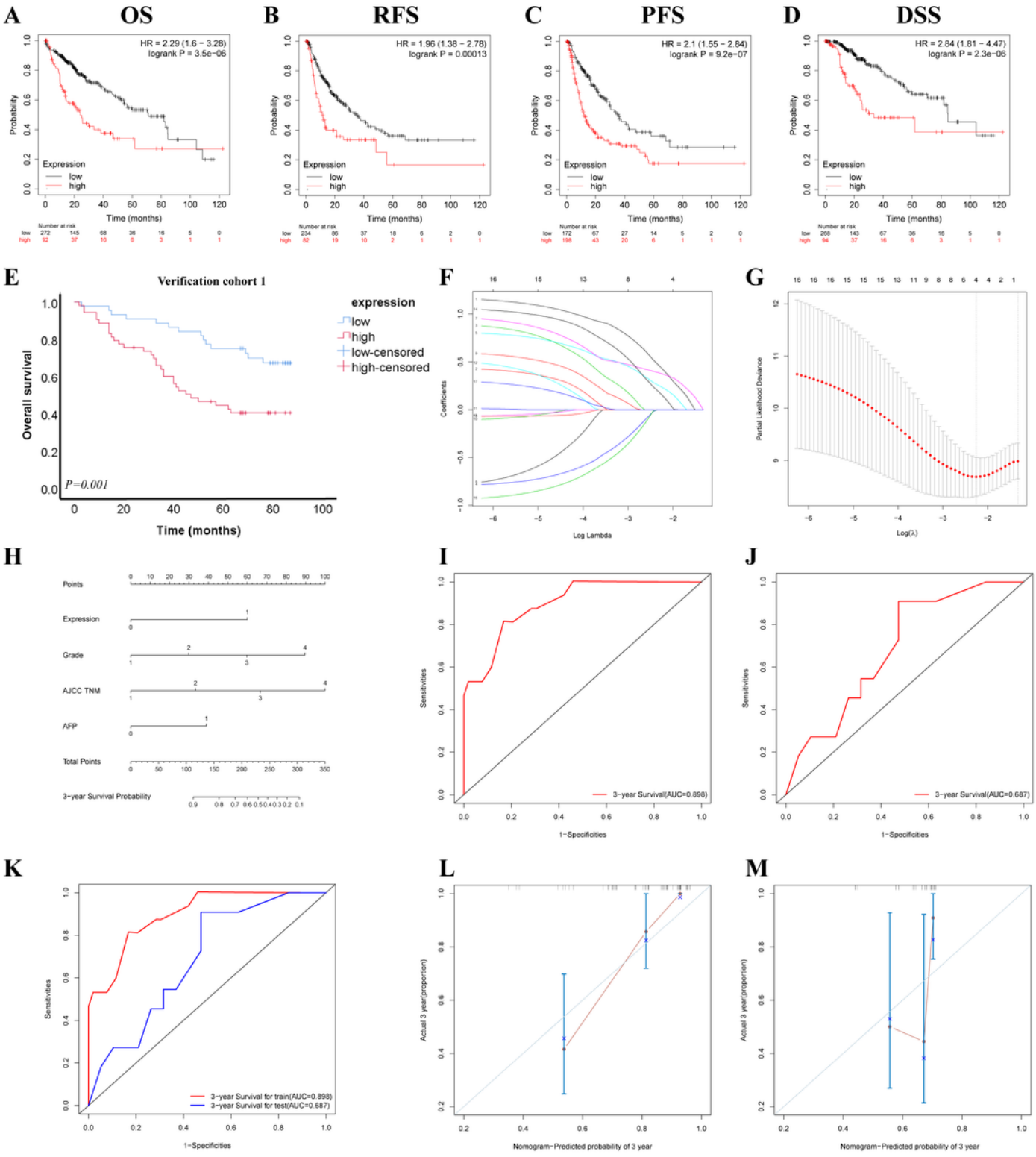

Figure 3

High expression of SGOL2 indicated the bad prognosis of HCC patients. A-D, Graphs generated from the Kaplan-Meier Plotter database show the prognostic values of SGOL2 in HCC patients. E, The overall survival (OS) analysis of the HCC patients with high SGOL2 expression or low SGOL2 expression in cohort 1. F-G, Identification of the optimal penalization coefficient lambda (λ) in the Lasso model. H, The nomogram based on SGOL2 for predicting the prognosis of HCC patients. I-K, ROC was used to evaluate

the performance of this nomogram for 3-year overall survival prediction in training and validation groups. L-M, 3-year calibration curve in the training (left) and validation groups (right). OS, overall survival; RFS, relapse-free survival; PFS, progression-free survival; DSS, disease-specific survival; HR, hazard ratio.

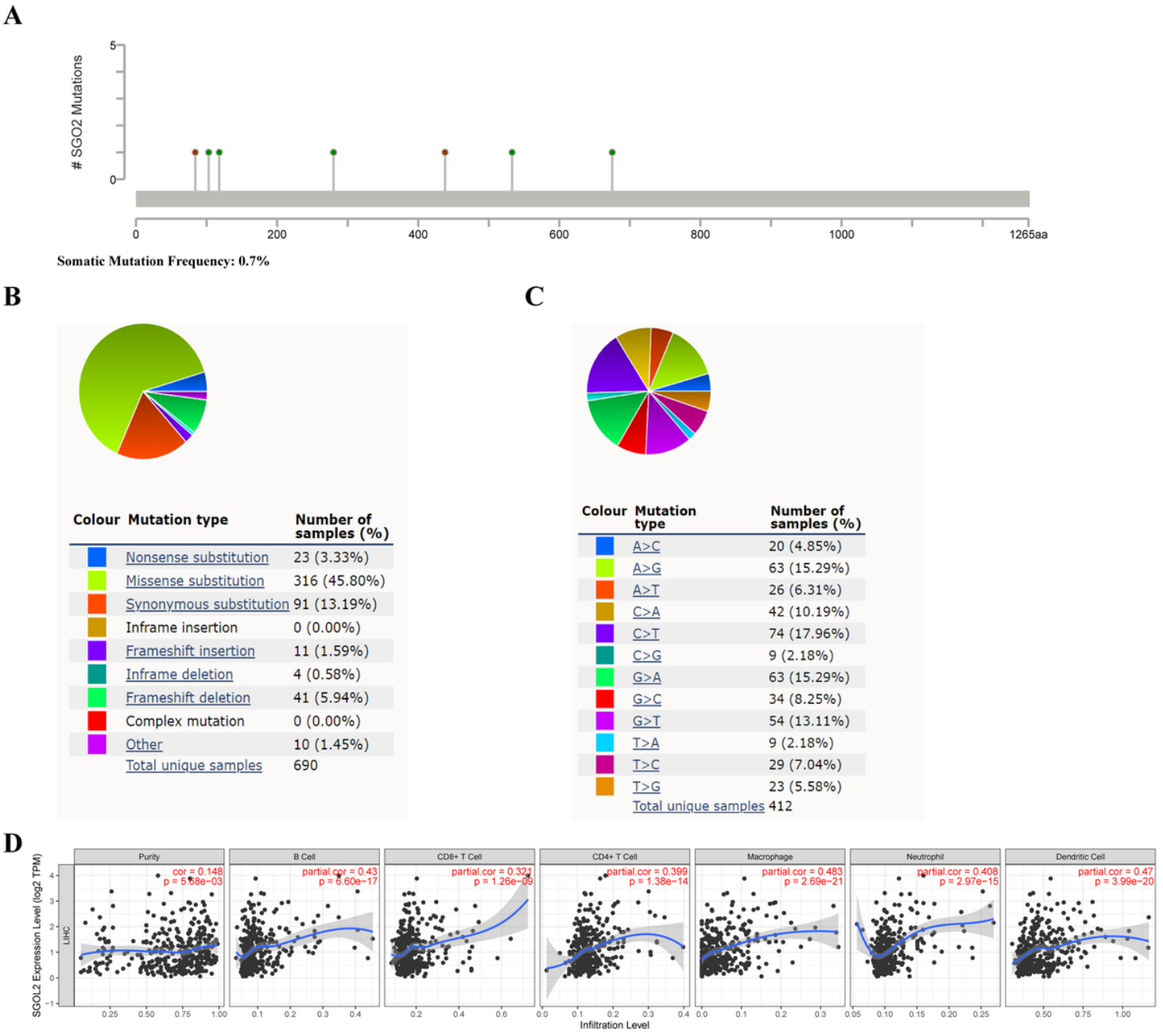

Figure 4

SGOL2 mutations and the correlations between SGOL2 and immune cell infiltrations in HCC. A, The representation of SGOL2 mutations in HCC (cBioPortal). B-C, The mutation types in HCC (COSMIC); D, SGOL2 is associated with immune infiltration in HCC (TIMER).

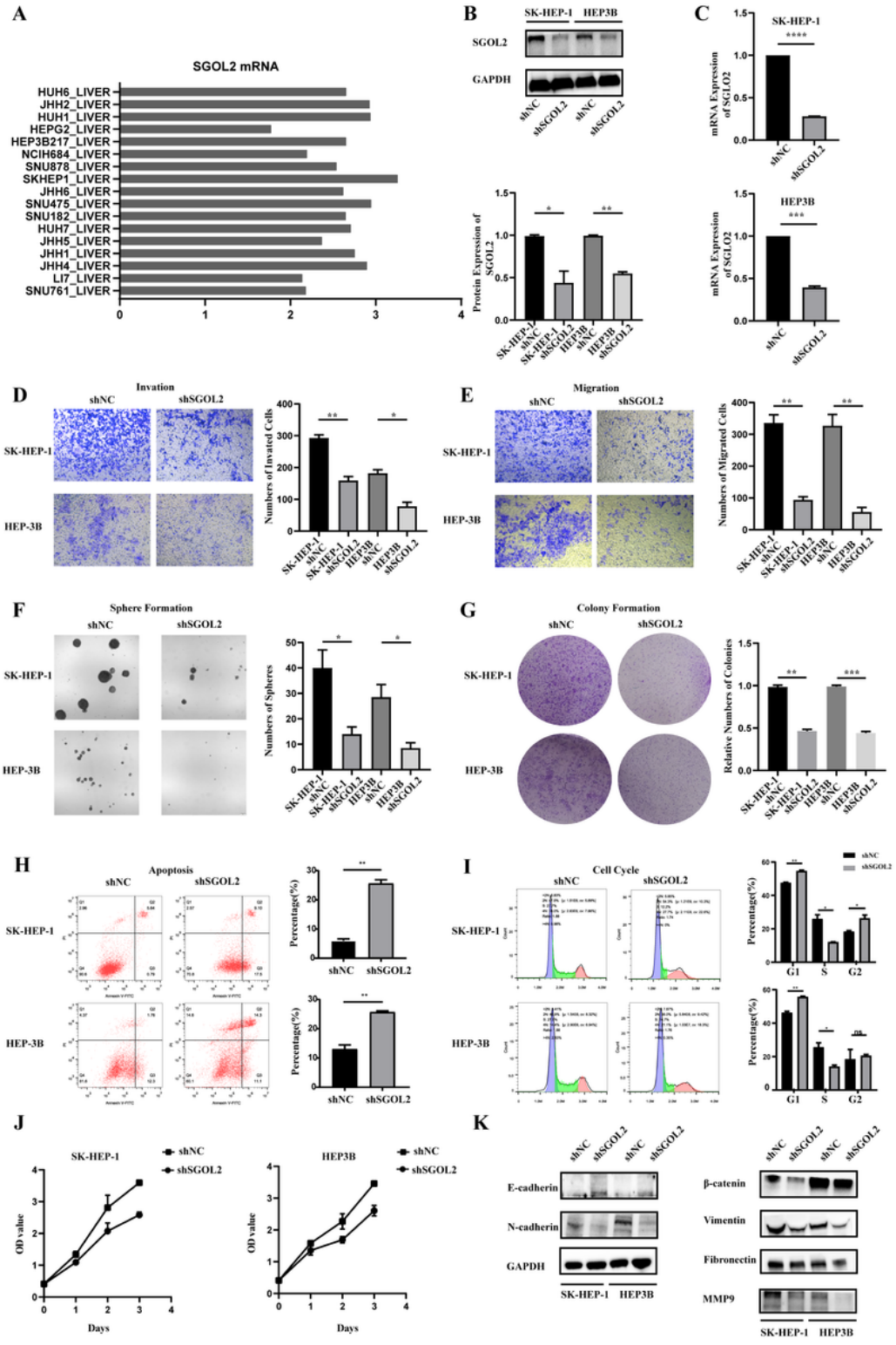

Figure 5

Downregulation of SGOL2 inhibited the malignant behaviors of HCC cells in vitro. A, The mRNA level of SGOL2 in liver and HCC cell lines. B-C, SK-HEP-1 and HEP3B cells were transfected with shNC or shSGOL2 lentivirus, and the knockdown of SGOL2 in mRNA and protein levels were validated by RT-PCR and western blot respectively. D-G, Invasion assay, Migration assay, sphere formation and colony formation of the SGOL2-downregulated HCC cells were detected and analyzed. H-I, Downregulation of

SGOL2 induced cell cycle arrest in G1/S phase and activated the apoptosis of HCC cells. J, SK-HEP-1 and HEP3B cells were transfected with shNC or shSGOL2, and the proliferation of HCC cells was detected at day 0, 1, 2, 3 by CCK-8. K, K-HEP-1 and HEP3B cells were transfected with shNC or shSGOL2, and the levels of E-cadherin, N-cadherin, β-catenin, Vimentin, Fibronectin and MMP9 were detected by western blot. *P<0.05, **P<0.01, ***P<0.001, ****P<0.0001.

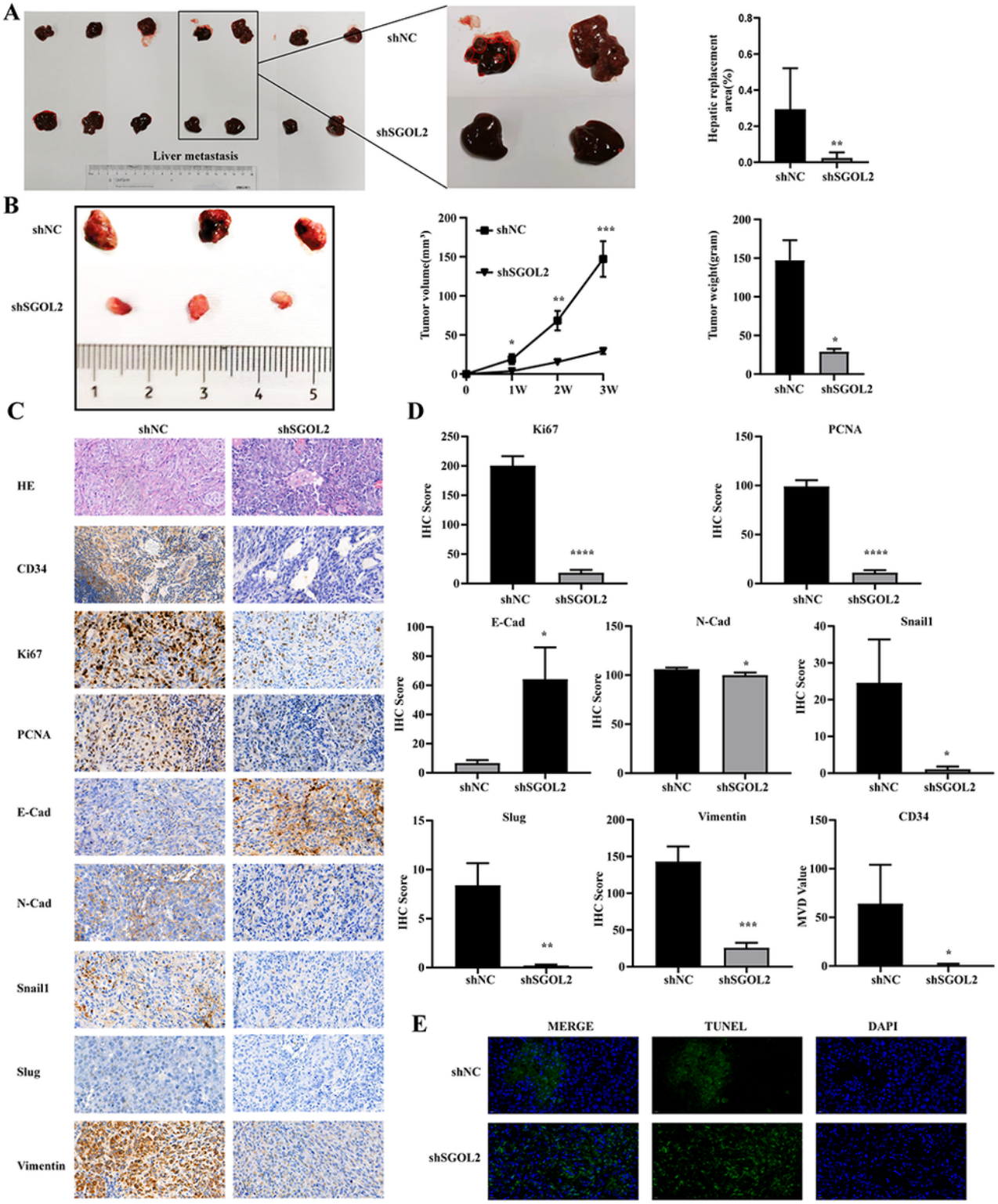

Figure 6

Downregulation of SGOL2 inhibited tumorigenicity and and promoted apoptosis in vivo. A-B, Mice were divided into two groups and were inoculated with SK-HEP-1 shNC or SK-HEP-1 shSGOL2 cells respectively. The images of the isolated livers and tumors from sacrificed mice were presented, and the hepatic replacement area (HRA%), the tumor volumes and tumor weights of the indicated groups were analyzed and compared. Loss of SGOL2 in SK-HEP-1 contributed to the reduction of tumorigenesis. C-D, IHC staining of CD34, Ki-67, PCNA, and EMT-related markers. Representative images and quantitative analysis results are shown. E, Apoptotic area was dramatically increased in shSGOL2 group compared with shNC group.

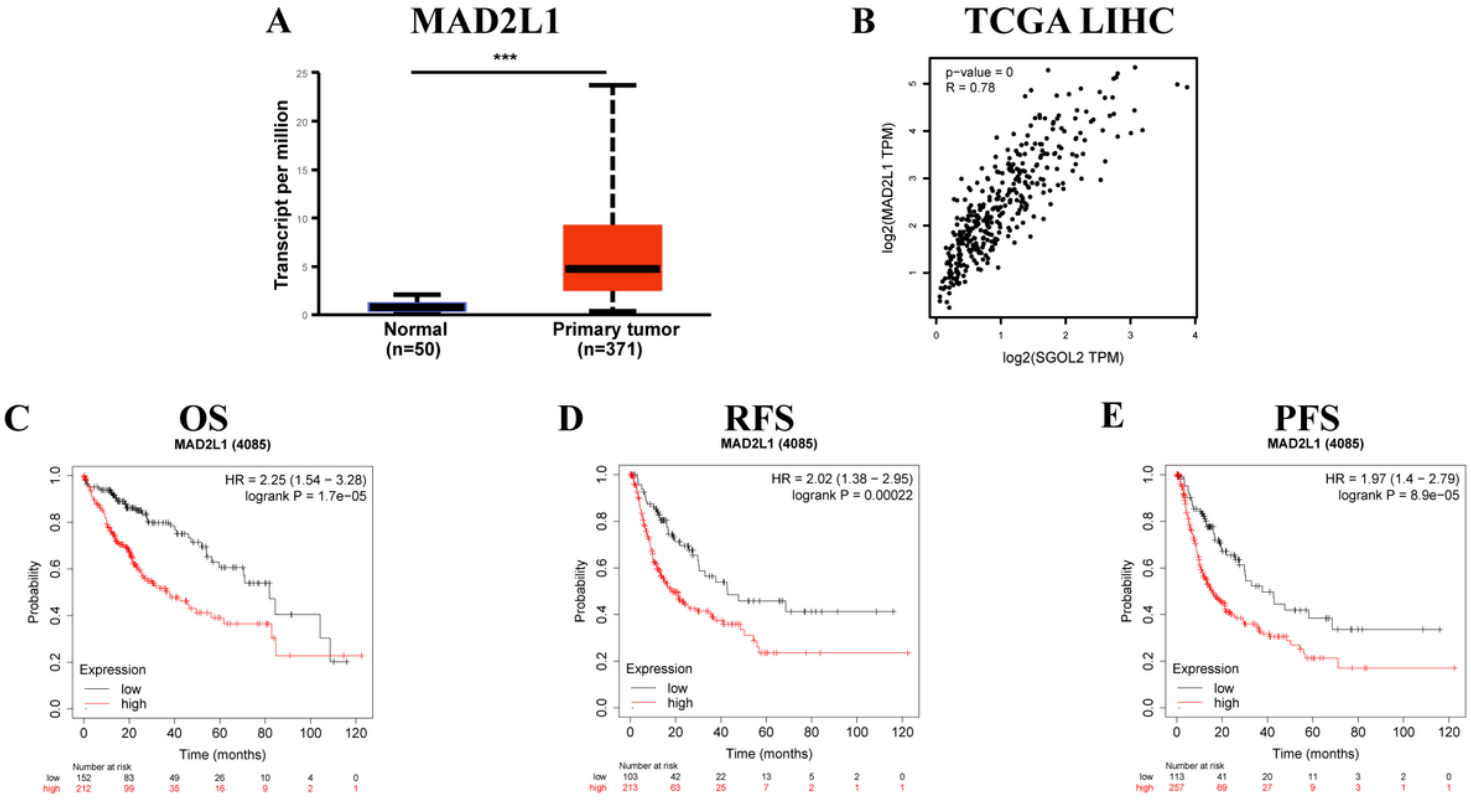

Figure 7

Upregulated MAD2 predicted poor prognosis in HCC. A, MAD2 mRNA express is overexpressed in HCC (UALCAN). B, MAD2 is positively correlated with SGOL2 in HCC (GEPIA). C-E, High MAD2 expression predicts poor OS, RFS and PFS in HCC. HR: hazard ratio

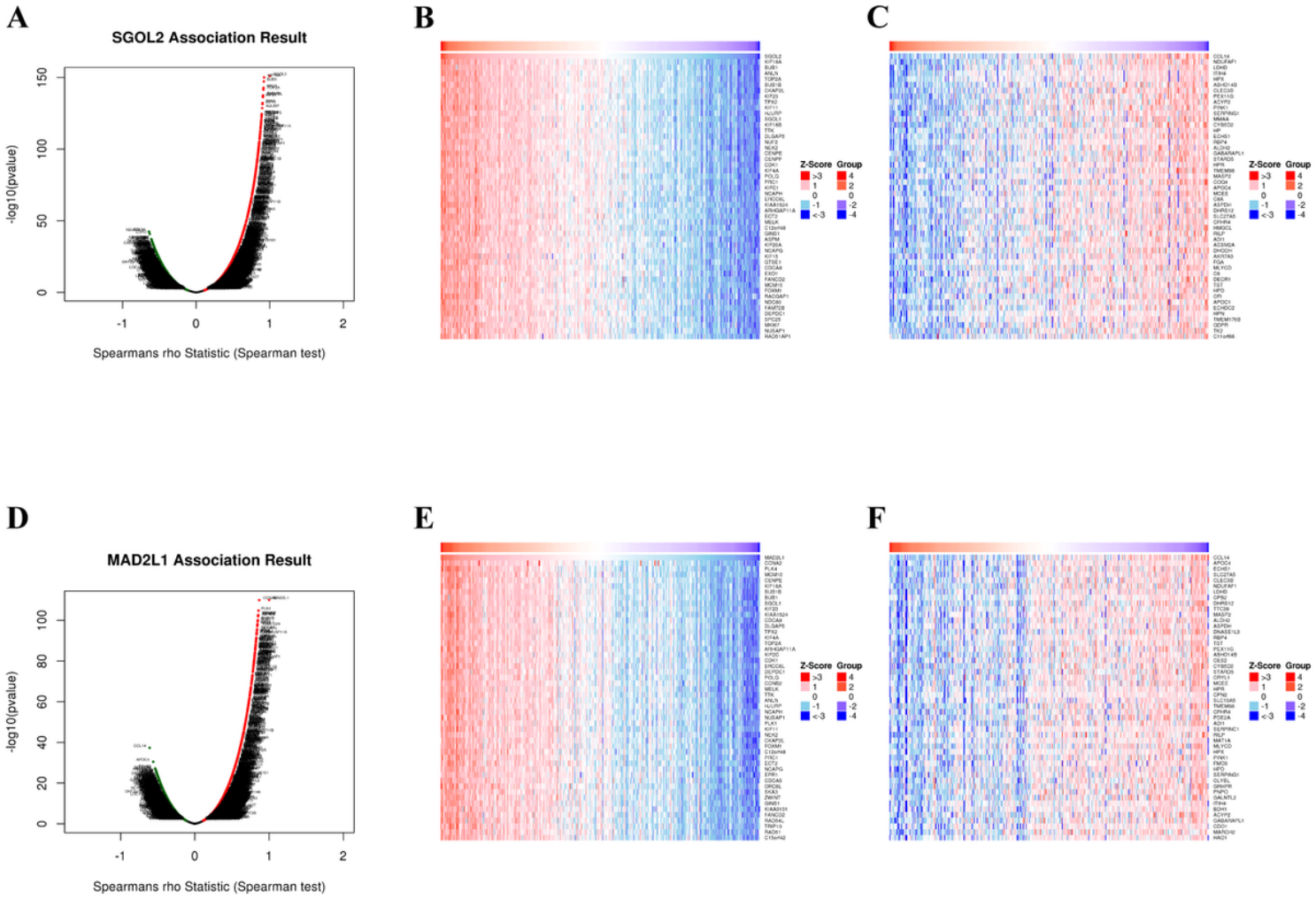

Figure 8

Differentially expressed genes that correlated with SGOL2 or MAD2 in HCC. A, Differentially expressed genes related to SGOL2. B-C, Genes positively or negatively related to SGOL2 (Top 50). D, Differentially expressed genes related to MAD2. E-F, Genes positively or negatively related to MAD2 (Top 50).

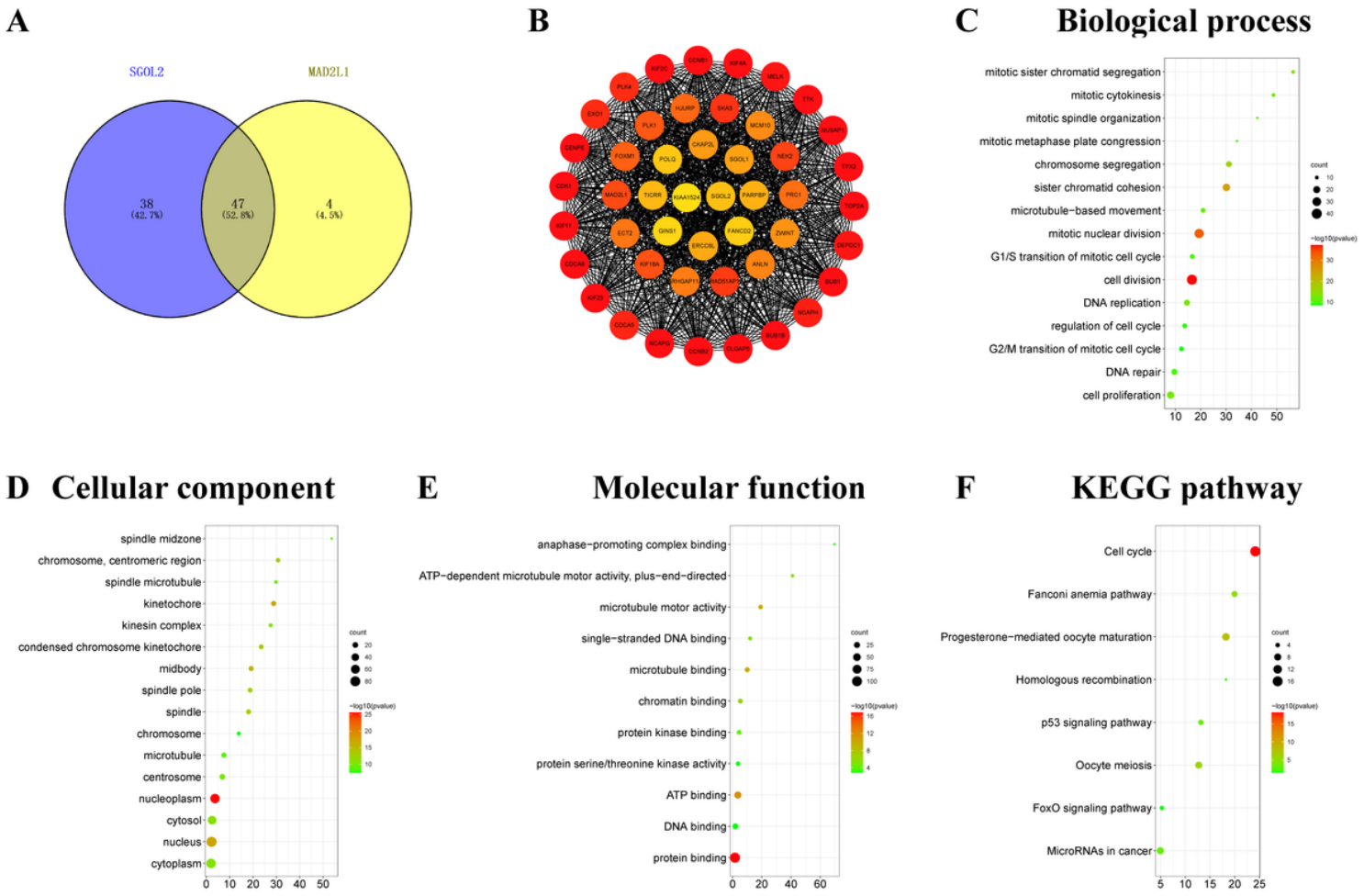

Figure 9

Functional analysis of genes positively correlated with both SGOL2 and MAD2. A, 47 genes are positively correlated with both SGOL2 and MAD2 were showed by venn results. B, The interaction network of the 47 genes. C-F, GO analysis and KEGG enrichment of the 47 genes.

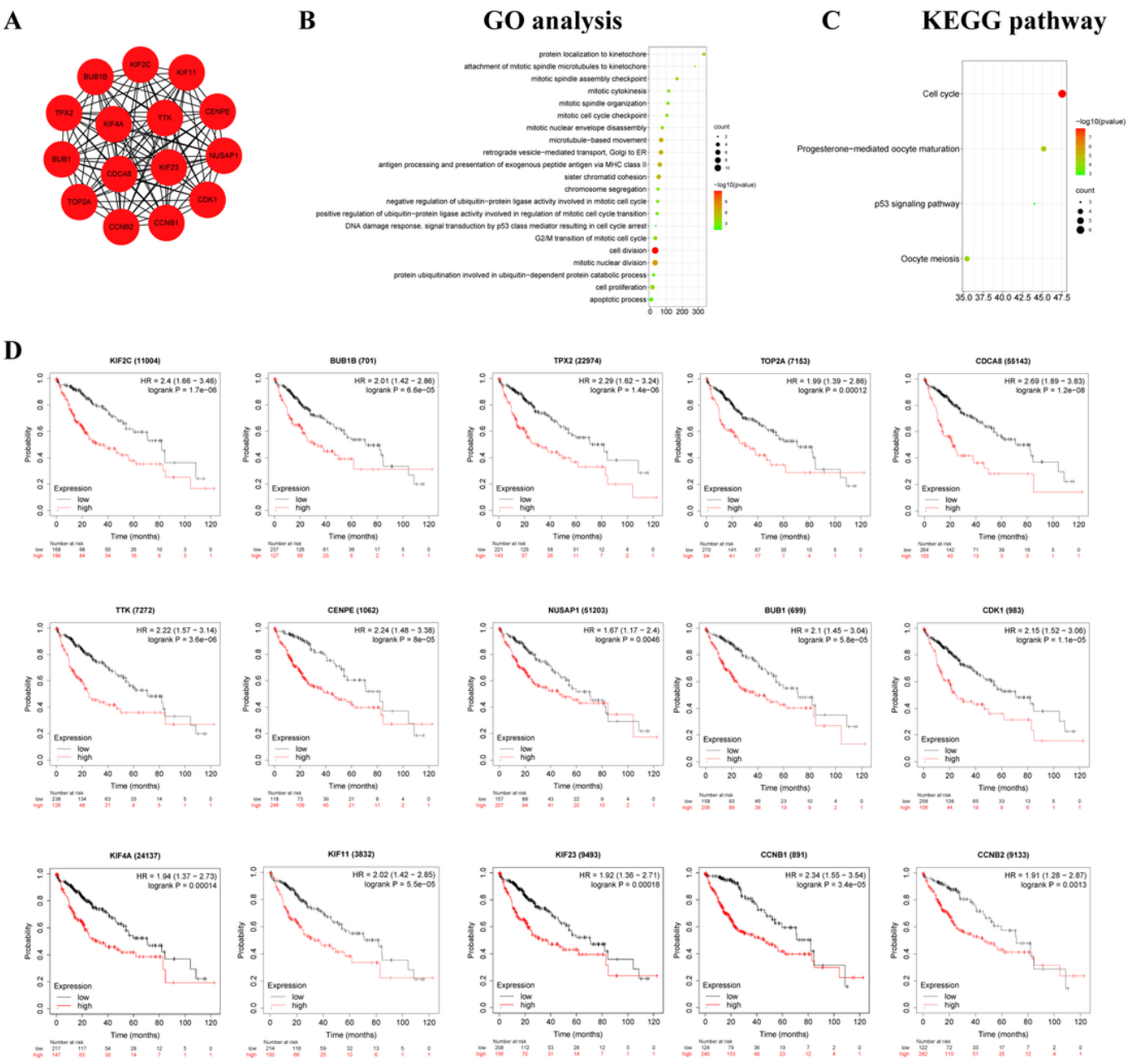

Figure 10

Hub gene analysis. A, The interaction network of the top 15 hub genes. B-C, GO analysis and KEGG enrichment of the top 15 hub genes. D, The prognostic values of the top 15 hub genes.

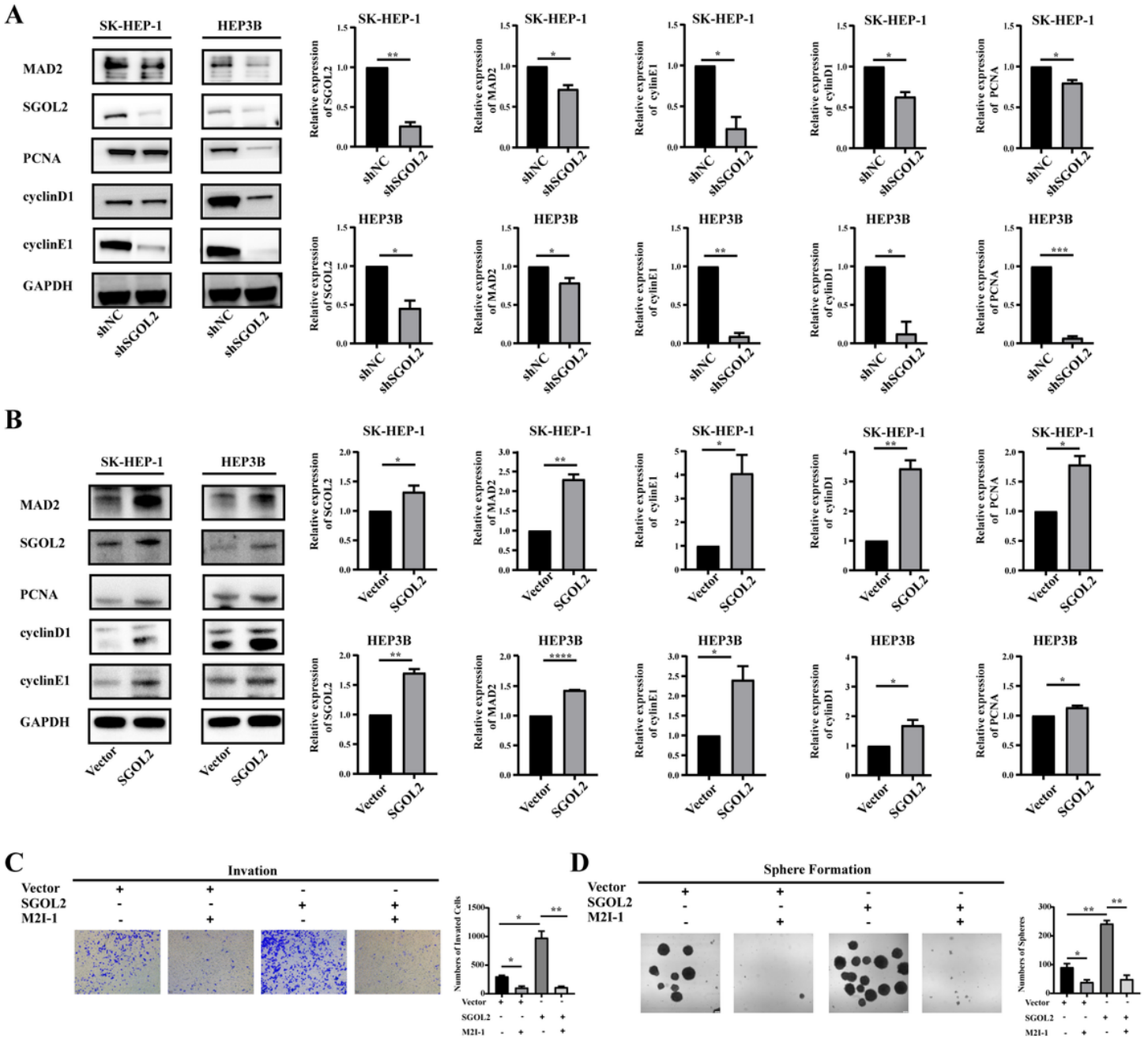

Figure 11

SGOL2 dysregulated cell cycle via promoting the activation of MAD2 in HCC cells. A, SK-HEP-1 and HEP3B cells were transfected with shNC or shSGOL2, and the levels of PCNA, cyclin D1, cyclin E1, SGOL2 and MAD2 were detected by western blot. B, SK-HEP-1 and HEP3B cells were transfected with SGOL2 plasmid or vector control plasmid, and the levels of PCNA, cyclin D1, cyclin E1, SGOL2 and MAD2 were detected by western blot. C-D, Invasion assay and sphere formation of the SGOL2-upregulated HCC cells with M2I-1 treatment were detected and analyzed. *P<0.05, **P<0.01, ***P<0.001, ****P<0.0001.

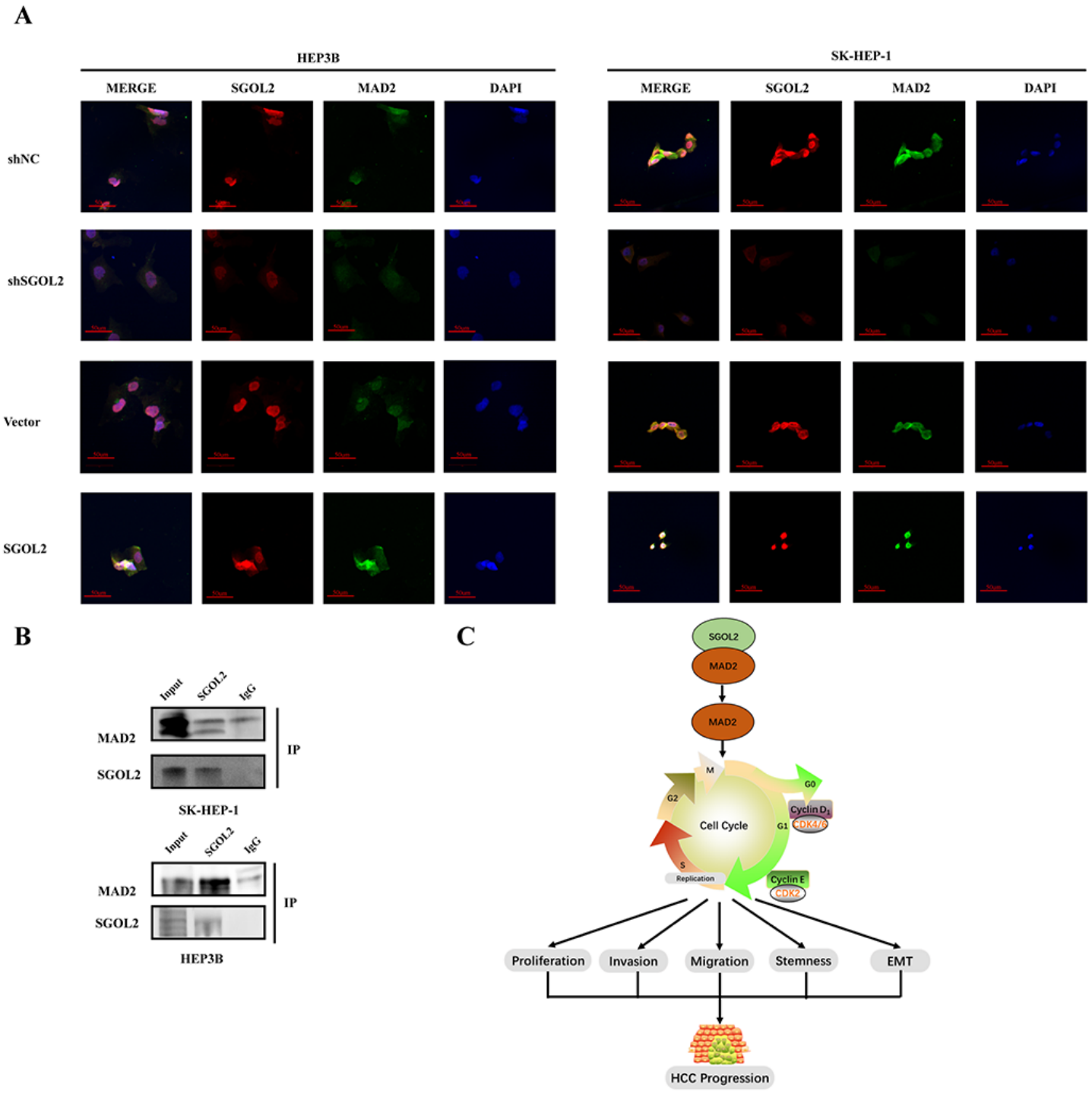

Figure 12

SGOL2 exerted its effect by directly interacting with MAD2. A, The co-localization between SGOL2 and MAD2 was visualized as yellow fluorescence in the merged panel. B, The endogenous interaction between SGOL2 and MAD2 were detected by IP assay in HCC cells. C, The role and mechanism of SGOL2 in HCC cells. SGOL2 directly binds with MAD2 and further activates MAD2, resulting in the dysregulation of cell cycle and finally enhances HCC malignant behaviors.

Supplementary Files

This is a list of supplementary files associated with this preprint. Click to download.

- SupplementTables.docx